

# Osteoarthritis and Cartilage



## Differences in structural and pain phenotypes in the sodium monoiodoacetate and meniscal transection models of osteoarthritis



P.I. Mapp †‡\*, D.R. Sagar †§, S. Ashraf †‡, J.J. Burston †§, S. Suri †, V. Chapman †§, D.A. Walsh †‡

† Arthritis Research UK Pain Centre, University of Nottingham, UK

‡ School of Clinical Sciences, Clinical Sciences Building, City Hospital, Hucknall Road, Nottingham NG5 1PB, UK

§ School of Biomedical Sciences, Queens Medical Centre, University of Nottingham, Nottingham NG7 2UH, UK

### ARTICLE INFO

#### Article history:

Received 16 January 2013

Accepted 19 June 2013

#### Keywords:

Osteoarthritis  
Animal models  
Pain  
Inflammation  
Glucocorticosteroids

### SUMMARY

**Objectives:** To characterize differences in joint pathology and pain behavior between two rat models of osteoarthritis (OA) in order to inform selection of animal models for interventional studies.

**Method:** Knee OA was induced in Sprague Dawley rats by either meniscal transection (MNX) or intra-articular injection of monosodium iodoacetate (MIA). Controls were subjected to sham surgery or saline-injection. In a separate experiment, a single intra-articular injection of triamcinolone acetonide was administered 14 days after MNX or MIA arthritis induction. Pain behavior and joint pathology were quantified.

**Results:** Both models displayed synovial inflammation, chondropathy and osteophytosis. Chondropathy scores increased with time similarly in the two models. Inflammation and osteophyte scores were greater in MNX model compared to the MIA model. At day 49, the MNX model exhibited a greater number of channels crossing the osteochondral junction compared to all other groups. The MNX model exhibited greater weight bearing asymmetry compared to the MIA model, whereas the MIA model displayed more consistent hindpaw allodynia. Triamcinolone attenuated weight bearing asymmetry and distal allodynia to control levels in the MNX model, but distal allodynia was unaltered in the MIA model.

**Conclusions:** The comparison of the two models of OA in rats, using identical assessment tools has demonstrated that although both models display features of OA, there are differences between the models which may represent different aspects of human OA. Thus, model selection should be based on the pathological aspects of OA under investigation.

© 2013 Osteoarthritis Research Society International. Published by Elsevier Ltd. All rights reserved.

### Introduction

The presenting symptoms of osteoarthritis (OA) are chronic pain and disability. However, the associations between OA structural changes and pain are often weak, and are incompletely understood<sup>1,2</sup>. Current drug treatments for OA are often limited by adverse events and incomplete efficacy. Intra-articular injection of corticosteroids and the oral or topical application of non-steroidal anti-inflammatory drugs<sup>3</sup> may be helpful for some patients. This, together with imaging and pathological evidence, suggests an important contribution from inflammation to OA pain<sup>4</sup>. Back-translation of these findings to

animal models should permit the development of more specific and effective treatments for OA.

It is currently unknown to what extent models of OA reflect relationships between structure (including synovitis) and symptoms observed in human disease. OA models have often been developed to explore mechanisms of cartilage damage, and reports of synovitis and pain behavior are often limited. Furthermore, few studies report on more than one model, and it is difficult to identify studies that make direct comparisons between models undertaken concurrently within the same experiment, with animals randomized between models and assessed using identical methods. As such, OA model selection is typically a matter of model experience or following precedence, rather than based on the most relevant pathophysiological phenotype for the question in hand.

We have compared structural and pain phenotypes between two commonly used animal OA models induced by meniscal transection (MNX) and intra-articular injection of sodium

\* Address correspondence and reprint requests to: P.I. Mapp, Arthritis Research UK Pain Centre, Clinical Sciences Building, City Hospital, Hucknall Road, Nottingham NG5 1PB, UK. Tel: 44-(0)115-823-1758; Fax: 44-(0)115-823-1757.

E-mail address: Paul.Mapp@nottingham.ac.uk (P.I. Mapp).

monoiodoacetate (MIA). The MNX model is induced by the transection of the medial collateral ligament and subsequent full thickness cut made through the meniscus<sup>5–7</sup>. Pathological changes similar to post-traumatic human OA are believed to result from instability and incongruity between joint surfaces. The monosodium iodoacetate (MIA) model<sup>8–10</sup> is induced by intra-articular injection of the metabolic inhibitor MIA, which inhibits the enzyme glyceraldehyde-3-phosphate dehydrogenase and disrupts glycolysis, on which articular chondrocytes are obligately dependant, leading to cell death<sup>11,12</sup>.

We monitored pain behavior by two methods. Firstly, weight distribution, which has been shown to be reduced on the ipsilateral hind limb<sup>11</sup>. Secondly, by changes in mechanical paw withdrawal thresholds at a site distal to the injured joint, the foot pad<sup>9,13</sup>. Pain on weight bearing, and reduced pain pressure thresholds, are both features of human OA<sup>14</sup>. Distal reduced pain pressure thresholds may represent abnormal central pain processing.

To investigate the contribution of inflammation to pain behavior we have employed a commonly prescribed drug used in human OA, triamcinalone acetonide, which we administered by intra-articular injection in both models once pathological changes had become established.

We hypothesized that the two different rat models of OA mimic different aspects of the relationship between pain and joint structure that have been demonstrated in human OA, and aimed to characterize any such differences in order to permit the appropriate selection of animal models for interventional studies.

## Methods

### Animal models

Experiments were approved by the University of Nottingham Local Ethics Review Committee and performed under United Kingdom Home Office licence, using male Sprague Dawley rats of approximately 180 g (Charles River, Kent, UK). Rats were housed on a 12 h light/dark cycle with food and water *ad libitum*. Joint swelling was measured with digital electronic calipers (Mitutoyo, UK), with values representing difference in knee diameters (mm) between the experimental (left) and contralateral (right) knee joints.

### Study design

84 rats were randomly assigned to the following groups: MNX, Sham surgery, MIA and intra-articular injection of saline and eight animals per group ( $n = 4$  for saline) were sacrificed for the investigation of pathological changes at 14, 35 and 49 days after model induction. In a separate experiment, rats received a single intra-articular injection of triamcinalone acetonide Kenalog 40<sup>®</sup>, 1 mg/25  $\mu$ l (E.R Squibb & Sons Ltd, Uxbridge, UK) or vehicle control, 14 days after model induction. 48 rats ( $n = 8$  in each group) were randomly assigned to the following: MIA/vehicle, MIA/triamcinalone acetonide, saline/triamcinalone acetonide, MNX/vehicle, MNX/triamcinalone acetonide and Sham/triamcinalone acetonide. Vehicle control for the triamcinalone acetonide injection comprised of 10 ml sterile 0.9% saline containing 0.075 g sodium carboxymethyl cellulose, 90  $\mu$ l benzoyl peroxide and 4  $\mu$ l Tween 80 (all Sigma UK). In each experiment, rats from all experimental groups were from a single batch of rats and studied concurrently by the same observers blinded to experimental group. Each experimental measurement, e.g., weight bearing or paw withdrawal threshold, was made by the same observer in both models. Rats were sacrificed at 21 days after model induction.

### Induction of MNX model

The MNX model of arthritis was induced as previously described<sup>5</sup>. Rats were anaesthetized using 2.5% Isoflurane (Abbott, Maidenhead, UK) in oxygen with a flow rate of 1 L per minute. The left leg was shaved and surgically prepared. The medial collateral ligament was exposed and a section of it was removed to expose the meniscus. The meniscus was cut through its full thickness at the narrowest point. The connective tissue layer and skin were closed with coated Vicryl 8-0 and 4-0 sutures, respectively (Ethicon, Livingstone, UK). No post-operative analgesic drug was administered as pain behavior was an outcome measure of the experiment. Sham operated animals underwent an identical procedure with the exception that the meniscus was not transected.

### Induction of MIA model

The MIA model of arthritis was induced as previously described<sup>5,15</sup>. Rats received a single intra-articular injection of monosodium iodoacetate (1 mg in 50  $\mu$ l sterile saline, Sigma UK) through the infra-patella ligament of the left knee. Control rats received intra-articular injection of saline (50  $\mu$ l).

### Triamcinalone acetonide intervention study

OA pathology and pain behavior were allowed to develop for a period of 14 days after model induction, a time point at which the pathological features of inflammation, chondropathy and osteophyte formation are established. A single injection of 1 mg triamcinalone acetonide was then given into the left knee, the equivalent dose in mg/kg as that used in human treatment.

Baseline behavioral pain measurements were made prior to model induction and then at day 7, 14 (prior to steroid injection), 15, and 21 days. Animals were sacrificed 21 days after arthritis induction (7 days after intra-articular triamcinalone acetonide administration).

In both studies, the animals were sacrificed by exposure to a slowly rising concentration of carbon dioxide.

### Histology

For each rat, skin was removed and the tibiofemoral joints were isolated by cutting mid-femur and tibia. The intact joints were preserved in neutral buffered formalin (containing 4% formaldehyde) for 48–72 h and subsequently decalcified in neutral buffered formalin containing 10% formic acid for approximately 10 days. Each joint was split by frontal sectioning and embedded to give an anterior and posterior block. Coronal sections (5  $\mu$ m), were taken through each of the wax blocks and stained with either hematoxylin and eosin, or safranin O. Sections were selected to give an approximate spacing of 200  $\mu$ m as recommended by the OARSI histopathology initiative<sup>16</sup>.

For the triamcinalone acetonide interventional experiment, the synovium was removed prior to fixation and snap frozen before subsequent storage at  $-80^{\circ}\text{C}$ .

### Histomorphometry and pathology scoring

The pathology scoring was performed on H/E sections with the exception of chondropathy which was done on Safranin O stained sections.

Osteophytosis and chondropathy were evaluated by the method of Janusz<sup>5</sup>. Osteophytosis was scored on a scale of 0–3, follows: 0. No osteophyte present; 1. Mild, <50  $\mu$ m; 2. Moderate, 50–150  $\mu$ m; and 3. Severe, >150  $\mu$ m. Chondropathy was scored on a scale of 0–5 as follows: 0. Cartilage of normal appearance; 1. Minimal fibrillation, superficial zone only; 2. Mild, extends to the upper middle

zone; 3. Moderate, well into the middle zone; 4. Marked, into the deep zone but not to the tidemark; and 5. Severe, full thickness degeneration to tidemark. Cartilage damage was estimated as the proportion of the section of the medial tibial plateaux involved, 1/3, 2/3 or 3/3 and the cartilage score multiplied by 1, 2 or 3 respectively to give a total chondropathy score.

Osteochondral vascular density was determined by counting the number of blood vessels crossing the osteochondral junction in the entire medial tibial plateau of mid-coronal sections<sup>6</sup>. An arithmetic mean was determined for three sections from each knee. A geometric mean ( $\pm 95\%$  confidence intervals) was then calculated for each group of animals.

Synovial inflammation was scored according to the thickness of the synovial lining layer and synovial cellularity in the medial and lateral tibiofemoral compartment<sup>6</sup>,

0	Lining cell layer 1–2 cells thick
1	Lining cell layer 3–5 cells thick
2	Lining cell layer 6–8 cells thick and/or mild increase in cellularity.
3	Lining cell layer >9 cells thick and/or severe increase in cellularity.

All measurements were made blinded to treatment group or surgical procedure, and with sections in random order. Each experimental measurement, histological and behavioral, was made by the same observer in both models.

#### Pain behavior

Effects of treatments on weight distribution through the left (ipsilateral) and right (contralateral) knees were assessed using an incapitance meter (Linton Instruments UK) as previously described<sup>11</sup>. The change in hindpaw weight distribution was defined as the difference in the amount of weight between the right contralateral control limb and the left ipsilateral treated limb divided by the sum of the weight right and left limbs  $\times 100$ .

Hindpaw withdrawal thresholds to mechanical stimulation were measured using calibrated von Frey monofilaments using the up down method, as previous described<sup>17</sup>.

The animals were habituated on at least two occasions before commencement of the experiments. Baseline behavioral pain measurements were made at day 0 prior to model induction and then at day 14, 28, 35, and 49 days.

#### Statistical analysis

Statistical analyses used Statistical Package for the Social Sciences v.14 (SPSS inc., Chicago, Illinois). Differences between groups were determined using one way ANOVA followed by post hoc *t*-tests with Bonferroni's corrections on parametric (normally distributed) data. Tests for normal distribution were made using the Kolmogorov–Smirnov test. Differences between groups in which the data were not parametric were determined using the Kruskal–Wallis test with post hoc Mann–Whitney analysis. The data are presented in the text as means and the degree of uncertainty as 95% confidence intervals for parametric data and medians with interquartile ranges for non-parametric data. A two-tailed *P* value of <0.05 was taken to indicate statistical significance.

Graphs were constructed using Prism v 4 (GraphPad, San Diego CA), as Mean  $\pm$  S.E.M.

## Results

### Structural changes to the joint

Both of the models of OA displayed histologic features characteristic of the clinical features of the disease [Fig. 1(a) and (b)]. Both

MNX rats and MIA-treated rats displayed chondrocyte degeneration, loss of surface integrity of the articular cartilage, osteophytosis and synovial hyperplasia.

### Synovial inflammation

Intra-articular injection of MIA did not alter the knee diameter of the injected knee compared to the contralateral knee, and there were no significant differences between knee diameters for the MIA-injected and saline-injected rats at any time point. Both the MNX-operated knee and the sham-operated knee exhibited a small increase in knee diameter (means 0.05 (0.39–0.62) mm and 0.4 (0.28–0.52) mm respectively at day 7), compared with contralateral control knees. The difference in the increase in knee diameters between MNX and sham controls was not statistically significant. Diameters of MNX- and sham-operated knees returned to control contralateral values by day 28.

For each model and at each time point, the synovial inflammation score was greater in the arthritic model than in the respective control [Fig. 2(A)]. The MNX model exhibited higher synovial inflammation scores than did the MIA model at each time point. Synovial inflammation scores did not differ significantly over time in either model.

### Osteophytosis

At day 49, osteophyte scores [Fig. 2(B)] were greater in the MNX model (median = 2.0 (IQR = 1.0–2.0)) than sham controls (median = 0.0 (IQR 0–0), *P* < 0.01), and greater in the MIA model (median = 0.0 (IQR 0–2.5)) than in saline-injected controls (median = 0.0 (IQR 0–0) *P* < 0.01). Osteophyte scores were greater at all time points in the MNX model, compared to the MIA model.

### Chondropathy

Knee joint chondropathy scores increased in both models of OA over time [Fig. 2(C)]; scores did not differ between the MNX and the MIA model. At day 49, the chondropathy score in the MNX model (median = 15 (IQR 10–15)) was higher than the chondropathy score in the sham controls (median = 0.0 (IQR 0–0), *P* < 0.01). Similarly, the chondropathy score for the MIA model (median = 15 (IQR 0–15)) was higher than score in the saline controls (median = 0 (IQR 0–0) *P* < 0.01). Chondropathy scores correlated with weight bearing decrease only in the MNX model at day 49, Spearman's rho = 0.59, *P* < 0.05.

### Osteochondral channels

Greater numbers of channels crossed the osteochondral junction at day 49 in the MNX model (mean = 2.5 (1.1–3.9) channels/mm) compared to sham controls (mean = 1.0 (0.3–1.6)), and compared to the MIA model (mean = 1.3 (1.0–1.7)) and saline controls (mean = 0.4 (–0.9 to 1.7) each *P* < 0.01). Whilst the number of osteochondral channels in sham controls, MIA model and saline controls decreased over time, numbers of osteochondral channels in the MNX model did not significantly decrease over time.

### Pain behavior

In the first experiment, greater weight bearing asymmetry was observed in the MNX model than in MIA-injected animals [Fig. 3(A) and (B)]. Weight bearing asymmetry in the MNX model increased with time such that there was a significant difference between MNX and sham controls at all time points after day 28. At day 49,

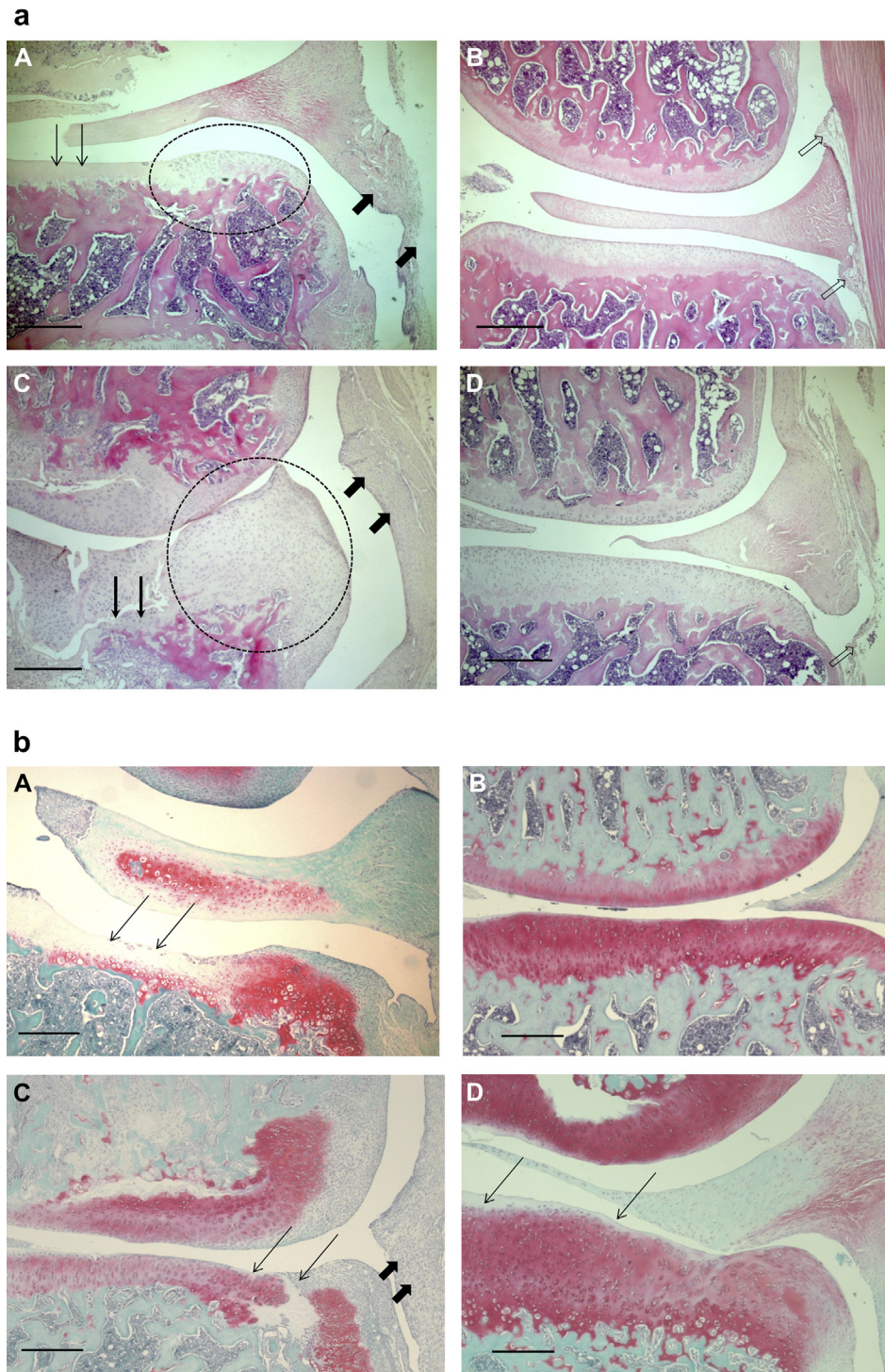


**Fig. 1.** a. Structural pathology in the two rat models of OA. MIA-injection (A) and MNX (C) were each followed by characteristic structural features of OA in medial tibial plateaux, whereas saline-injected (B) and Sham-operated (D) controls displayed normal morphology. Following MIA-injection (A) there was loss of chondrocytes in the articular cartilage (thin arrows) and a small osteophyte had formed on the medial edge of the plateau (oval area). Following MNX (C) there was extensive cartilage damage and erosion of the underlying bone (thin arrows). A large osteophyte (oval area) has formed on the medial aspect of the plateau. Synovia (thick arrows) in both models display inflammatory cell infiltrates. Saline-injected (B) and Sham-operated (D) knees, respectively controls for panels A and C, displayed medial tibial plateaux of normal appearance with chondrocytes throughout the depth of the cartilage. No osteophytes were seen, and synovium was also of normal appearance with only a thin layer of cells at the intimal surface (hollow arrows). Representative photomicrographs of sections with median values of measured histological features, taken from rats 49 days after model-induction. Scale bars 500  $\mu$ m. Hematoxylin and eosin stain. b. Safranin O staining for proteoglycans. Panel A showing extensive loss of proteoglycan in the cartilage in the MIA model particularly where chondrocytes are absent (thin arrows). Panel B saline control animal shows an even distribution of proteoglycan throughout the cartilage. Panel C shows loss proteoglycan in the MNX model together with disruption of the cartilage matrix (thin arrows) and inflammation in the synovium (thick arrows) Panel D a sham control animal shows minimal loss of proteoglycan on the cartilage surface. Representative photomicrographs of sections with median values of measured histological features, taken from rats 49 days after model-induction. Scale bars 500  $\mu$ m. Safranin O staining.

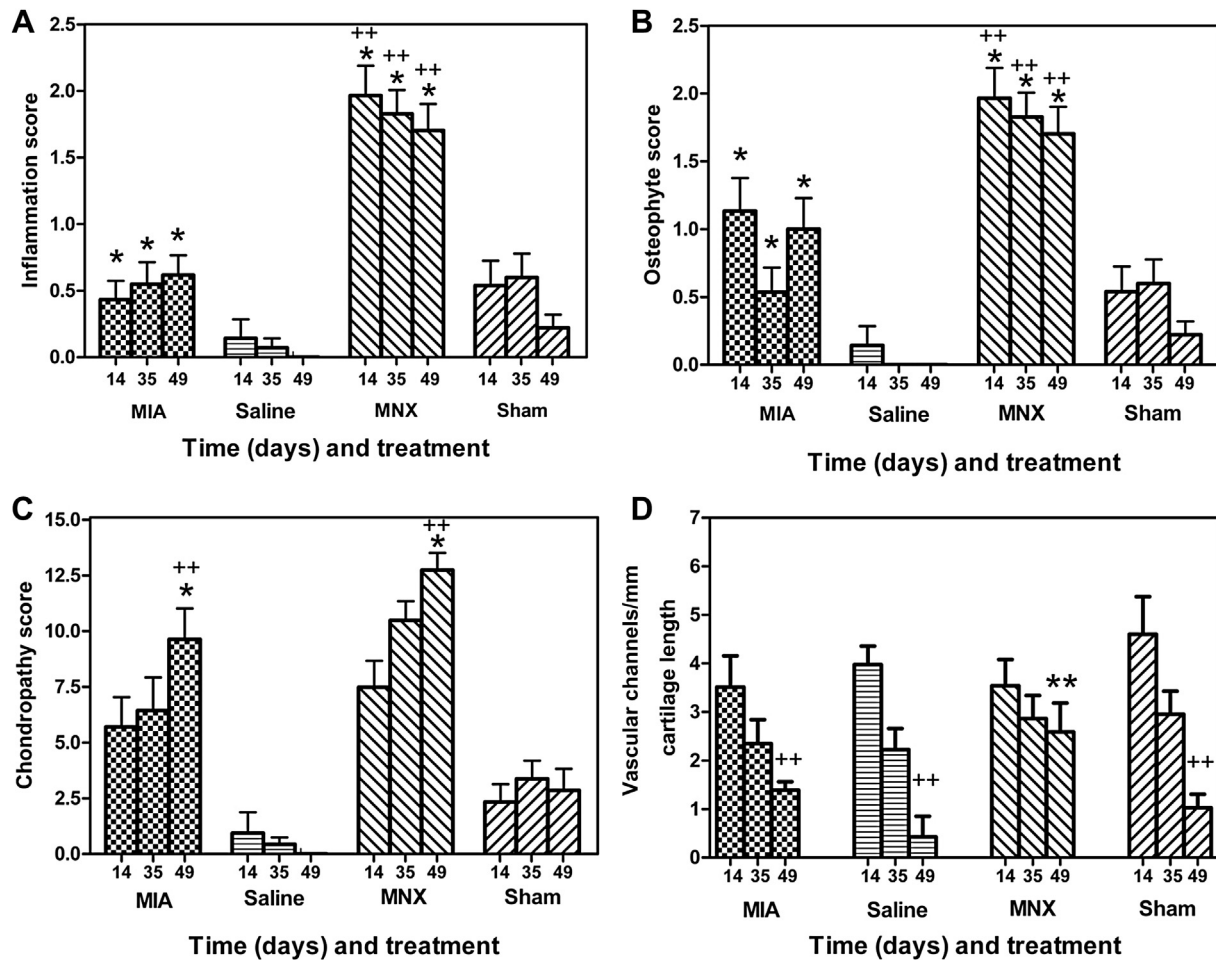


**Fig. 2.** Comparison of the extent of structural pathology between MIA and MNX models of OA over time from arthritis induction. The MNX model displayed greater synovitis (A) and osteophytosis (B) than did the MIA model. Chondropathy scores (C) were similar in the two models. In the MNX model, the normal decline in vascular breaching of the osteochondral junction was reduced (D). Inflammation (A) and osteophyte (B) scores were greater in arthritic knees from the MNX model than in the MIA model at corresponding time points (++)  $P < 0.01$ . In each model, inflammation and osteophyte scores were greater than in their respective controls (\*)  $P < 0.05$ . Inflammation and osteophyte scores did not differ significantly with time in any group. Chondropathy scores (C) increased with time when comparing day 14 to day 49 (\*\*)  $P < 0.05$  and did not differ significantly between MNX and MIA models. By day 49, arthritic knees had higher chondropathy scores than did their respective controls (++)  $P < 0.01$ . The density of channels crossing the osteochondral junction (D) decreased with time between days 14 and 49 in both saline-injected and Sham-operated rats. Similar reductions in osteochondral breaching were observed in the MIA model (++)  $P < 0.01$ . In contrast there was no significant decrease in osteochondral channels over time in the MNX animals, such that at day 49 the MNX model displayed greater numbers of channels crossing the osteochondral junction compared to Sham-operated controls, saline-injected controls and MIA-injected animals (\*\*)  $P < 0.01$ .

weight bearing asymmetry was mean = 10.9 (5.4–16.4)% in the MNX model compared to 0.2 (–3.7 to 4.3)% in sham controls.

MIA-injected rats did not display weight bearing asymmetry.

Mechanical withdrawal thresholds were measured in MNX and MIA-treated rats and their respective controls. There was a significant decrease in the hindpaw withdrawal threshold in the MIA model, compared to saline controls over the time course of the study [Fig. 3(C)]. Both the MNX model and the sham controls exhibited a small decrease in hindpaw mechanical withdrawal thresholds (significant only at day 14,  $P < 0.05$  compared to baseline) [Fig. 3(D)].

#### Effects of intra-articular triamcinolone acetonide injection on OA pathology and pain behavior

##### Synovial inflammation

Treatment with triamcinolone acetonide (1 mg) at day 14 [Fig. 4(A)] reduced synovial inflammation by day 21 in the MNX model (median inflammation score = 1 (IQR 1.0–1.0)) compared with vehicle-injected, MNX arthritic animals (median inflammation

score = 3 (IQR 2.5–3.0),  $P < 0.05$ ). Synovial inflammation following triamcinolone acetonide treatment in the MNX model was comparable to inflammation in the sham-operated, steroid-injected animals (median = 1.0 (IQR 1.0–1.0)). Similarly, intra-articular triamcinolone acetonide reduced synovial inflammation scores in the MIA model (median = 1.0 (IQR 1.0–1.0)) compared to the vehicle-injected MIA arthritic animals (median = 3.0 (IQR 3.0–3.0),  $P < 0.05$ ). Synovitis scores in triamcinolone acetonide-injected MIA arthritic animals remained slightly elevated compared with synovitis scores in the steroid-injected, non-arthritic controls (median = 0.0 (IQR 0.0–1.0),  $P < 0.05$ ).

##### Pain behavior

Weight bearing asymmetry was increased in the MNX model by day 14, compared with sham-operated controls, and more variably affected in the MIA model [Fig. 5(A) and (B)]. Intra-articular injection of triamcinolone acetonide on day 14 significantly reduced weight bearing asymmetry by day 21 in the MNX model (MNX/steroid mean = 0.22 (–2.6 to 2.6)% compared to MNX/vehicle mean = 7.8 (5.6–10.0)%,  $P < 0.001$ ).

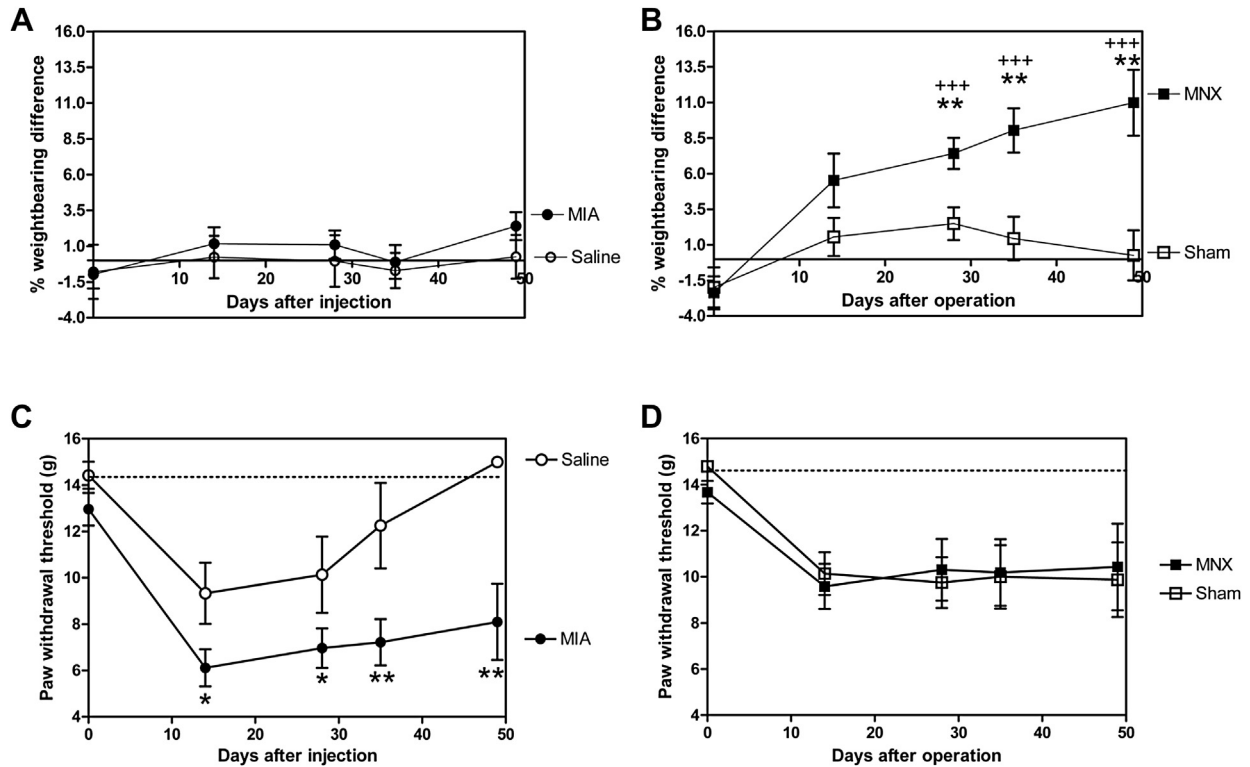


**Fig. 3.** Comparison of two measures of pain behavior in MIA- and MNX-induced models of OA over time. MIA (A and C) and MNX (B and D) models of OA were each associated with significant pain behavior as measured by either weight bearing asymmetry (A and B) or mechanical paw withdrawal thresholds to punctate stimulation (C and D). In this experiment, significant weight bearing asymmetry was not demonstrated in the MIA model (A) compared to saline-injected controls, whereas weight bearing asymmetry increased with time in the MNX model (B) compared to Sham-operated controls (\*\* $P < 0.01$ ). Weight bearing asymmetry was significantly greater in the MNX model than in MIA-injected rats at days 28, 35 and 49 (++++)  $P < 0.005$ . Mechanical paw withdrawal thresholds to punctate stimulation were reduced in MIA-injected animals (C) compared to saline-injected controls at all time points, (\* $P < 0.05$  at day 14 and 28 and (\*\* $P < 0.01$  at days 35 and 49). Saline-injected animals displayed transient reductions in mechanical paw withdrawal thresholds which returned to baseline values by day 35. Both MNX- and Sham-operated animals (D) showed decreased mechanical paw withdrawal thresholds at day 14 compared to baseline which did not further change with time. There were no significant differences in mechanical paw withdrawal thresholds between MNX- and Sham-operated animals in this experiment, nor between MNX-operated and MIA-injected animals at any time point.

In this experiment, paw withdrawal thresholds were decreased in both the MNX and the MIA models by day 14, compared with non-arthritic controls [Fig. 5(C) and (D)]. Intra-articular injection of triamcinolone acetonide at day 14 normalized the decrease in hindpaw withdrawal thresholds at day 21 in the MNX model [Fig. 5(D), MNX/steroid median = 12.5 (IQR 10.0–15.0) g as compared to MNX/vehicle median = 9.0 (IQR 8.0–9.0) g,  $P = 0.01$ ]. Intra-articular triamcinolone acetonide injection did not significantly alter hindpaw withdrawal thresholds in the MIA model [Fig. 5(C), MIA/steroid, median = 8.0 (IQR 8.0–9.0) g compared to MIA/vehicle median = 6.0 (IQR 5.0–7.0) g,  $P = 0.93$ ].

## Discussion

We have compared and contrasted two different models of OA, initiated in parallel and using protocols that minimized confounding by experimental factors other than the method of model induction. Both MIA and MNX models of OA in the rat displayed features that are comparable to human OA, including pain behavior, chondropathy, osteophytosis and synovial inflammation. In both models, osteophytosis and synovitis were evident at 14 days after model induction, and chondropathy progressively increased between 14 and 49 days after induction.

Despite these similarities, we also found differences between the two models that may indicate that they mimic different aspects of human disease. In particular, inflammation and osteophyte scores were greater in MNX- than in MIA-induced OA, and at day 49

MNX-induced OA displayed greater numbers of channels crossing the osteochondral junction compared to all other groups. Rats with MNX-induced OA displayed greater weight bearing asymmetry than after MIA-injection, whereas those with MIA-induced OA displayed more consistent lowering of the mechanical withdrawal thresholds of the hindpaw than after MNX.

We demonstrated synovial inflammation in both models. Synovitis is a feature of human knee OA<sup>18</sup>, in which it contributes to pain<sup>19</sup> and is associated with progressive joint damage<sup>20</sup>. Intra-articular injection of triamcinolone acetonide, an anti-inflammatory glucocorticosteroid, reduces pain in patients with knee OA, and we here confirm that intra-articular glucocorticosteroids may also reduce pain behavior in rodent models<sup>21</sup>. We found that synovitis was more pronounced in the MNX than the MIA-induced model of OA. Intra-articular triamcinolone acetonide injection had a greater effect on pain behavior in the MNX model, consistent with a greater contribution of synovitis to pain in the surgical model. We selected 14 days as a minimum time point at which OA changes become established and for ethical reasons to reduce the amount of time animals were in pain. A relative insensitivity of the MIA model to the cyclo-oxygenase inhibitors celecoxib and diclofenac has been reported<sup>13,22</sup>, particularly at late time points 18 days or more after model induction<sup>23</sup>.

Synovitis has been associated with cartilage damage and osteophyte formation both in man<sup>20</sup> and in a murine model of arthritis<sup>24</sup>. Osteophyte growth may be stimulated by transforming growth factor beta (TGF $\beta$ ), which is upregulated during synovitis<sup>25</sup>.

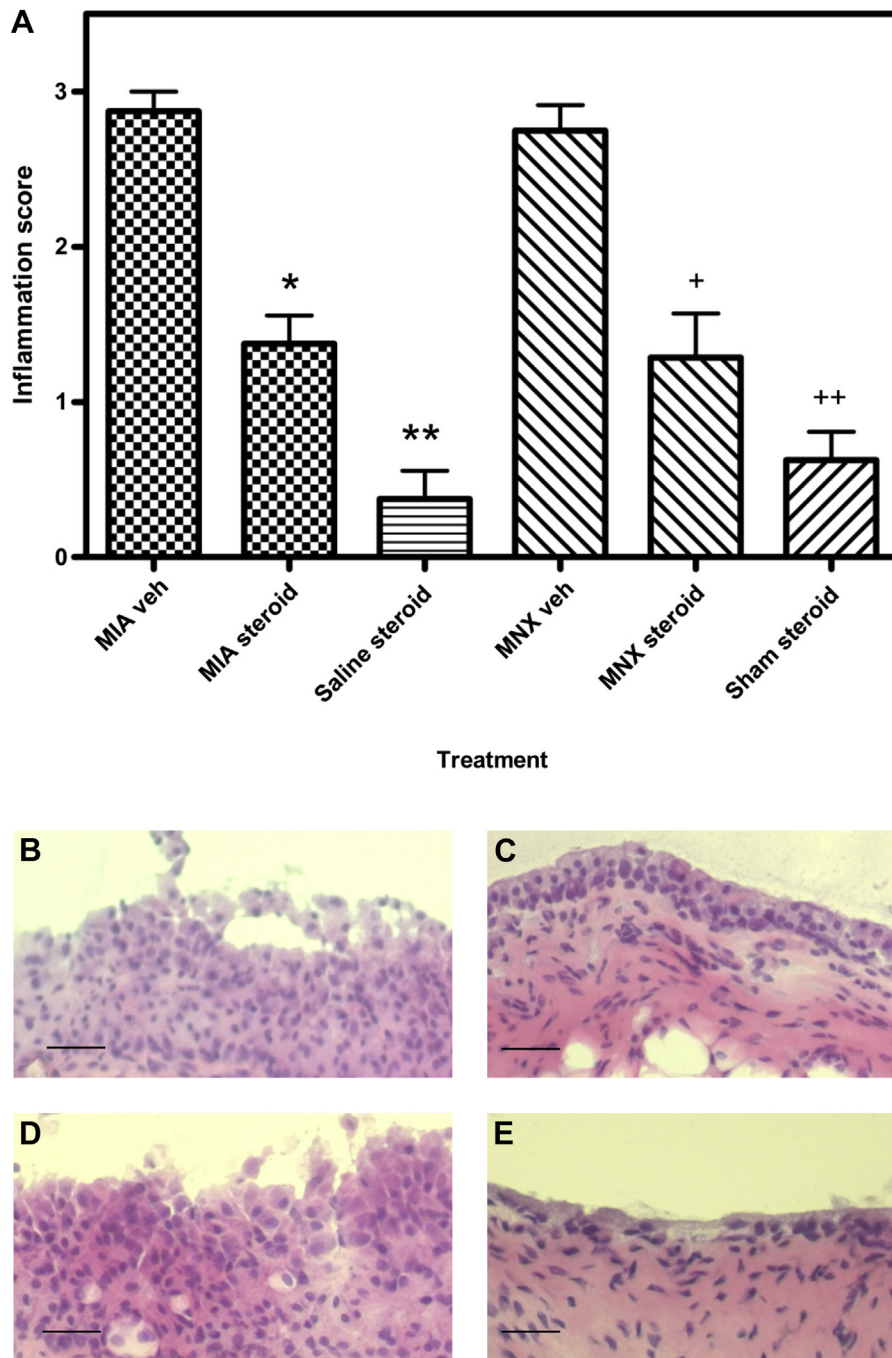


**Fig. 4.** Inflammation scores and synovial photomicrographs of MIA- and MNX-induced models of OA showing the effect of triamcinolone acetonide on the models seven days after treatment. A single administration of triamcinolone acetonide (steroid) reduced the inflammation scores in both the MIA and MNX model 7 days after the treatment when compared to vehicle treated controls. ( $P < 0.05$  in both cases). Representative photomicrographs of sections with median values of measured histological features, taken from rats 21 days after model-induction. Panel B MIA vehicle-treated, panel C MIA triamcinolone acetonide-treated. Panel D MNX vehicle-treated, panel E MNX triamcinolone acetonide-treated. Treatment reduces the overall thickness of the lining layer in both models. Scale bars 50  $\mu$ m. Hematoxylin and eosin stain.

Osteophytes are a potential source of OA pain because sensory nerves penetrate newly formed cartilage at the joint margins during osteophyte formation<sup>26</sup>. Synovitis may therefore contribute to OA pain both directly and by augmenting other aspects of OA structural pathology.

Vascular breaching of the osteochondral junction also distinguished between the two models in the current study. Normal adult human cartilage is avascular but in OA vascular growth occurs at the osteochondral junction<sup>26,27</sup>. We extend our previous findings

showing that osteochondral vascularity was higher in rats following MNX-surgery<sup>6</sup>, now showing that it was also greater in the MNX than MIA model. MIA-induced OA can, however, under some circumstances, also lead to increased numbers of osteochondral channels<sup>28</sup>. High osteochondral channel densities may indicate increased new channel formation<sup>29</sup> as they are reduced following treatment with the osteoclast inhibitor zoledronate<sup>28</sup>. Osteochondral channels in these immature animals displayed the normal decrease during maturation in control and MIA-injected

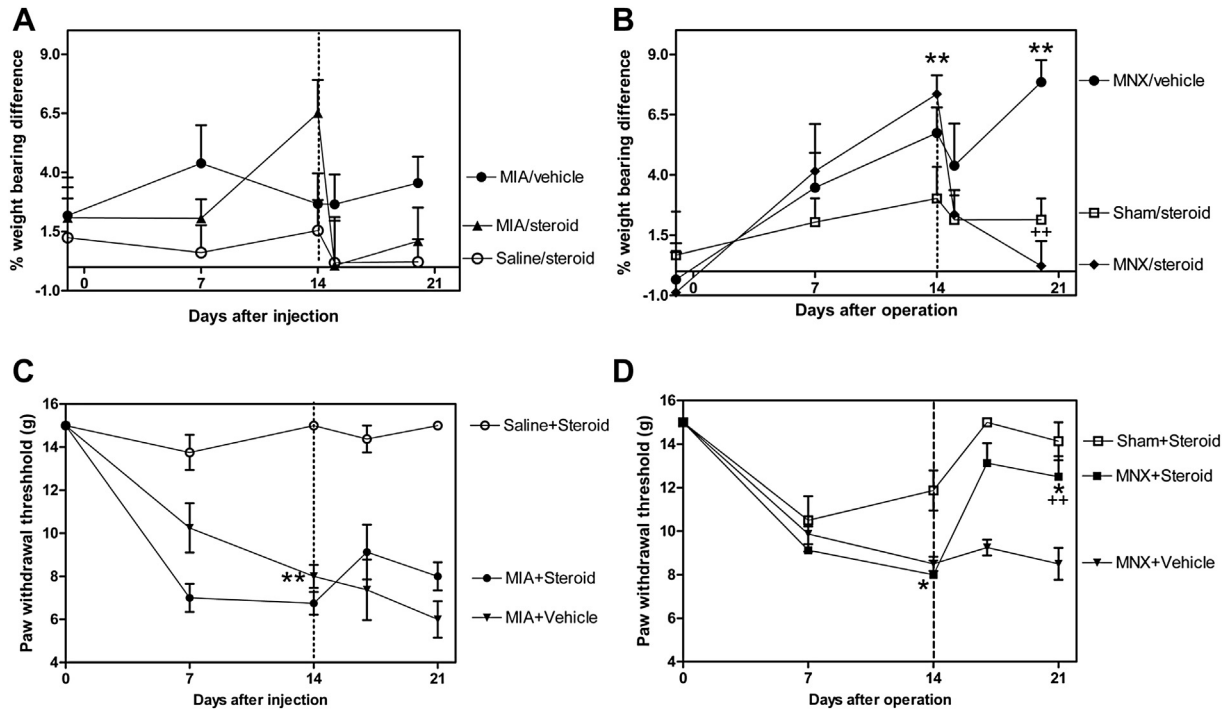


**Fig. 5.** Effects of intra-articular triamcinolone acetonide injection on pain behaviors in the monoiodoacetate (MIA) and MNX models. Intra-articular triamcinolone acetonide injections were administered in arthritic and control knees 14 days after model induction (dotted line) in the MIA- (A and C) and MNX-induced (B and D) models of OA, and effects on weight bearing asymmetry (A and B) and paw withdrawal thresholds to punctate stimulation (C and D) were determined. **Weight bearing asymmetry** was inconsistently increased by day 14 in the MIA model (A) and effects of steroid-injection did not reach statistical significance. (B) Weight bearing asymmetry was increased in MNX-operated animals compared to Sham-operated controls by day 14 (\*\* $P < 0.01$ ). Triamcinolone acetonide-injected, MNX-operated animals displayed a subsequent reduction in weight bearing asymmetry compared with vehicle-injected, MNX-operated arthritic controls (++)  $P < 0.01$  to levels that were not significantly different from steroid-treated, Sham-operated non-arthritic controls. (Error bars shown only above data points for clarity). **Paw withdrawal thresholds** were reduced 14 days after arthritis induction in both MIA (C) (++)  $P < 0.01$  and MNX (D) models (+)  $P < 0.05$  in this experiment when compared to non-arthritic controls. Intra-articular triamcinolone acetonide injection increased paw withdrawal thresholds in the MNX model when compared to MNX/vehicle controls (\* $P < 0.01$ ), and to levels similar to those observed in steroid-treated, Sham-operated (non-arthritic) controls. Intra-articular triamcinolone acetonide had no significant effect on paw withdrawal thresholds in the MIA model. At day 21, paw withdrawal thresholds were significantly greater in triamcinolone acetonide-injected, MNX-arthritic rats compared to steroid-injected, MIA-arthritic animals, (++)  $P < 0.01$ .

animals, and it is possible that the high osteochondral channel densities in MNX-induced OA resulted from original channels remaining open as well as from increased new channel formation. Increased osteochondral channel densities may be a source of pain by exposing subchondral nerves to abnormal stimulation<sup>30</sup>, or by permitting sensory nerve growth into the articular cartilage<sup>26</sup>.

We used two different methods to assess pain behavior. Weight bearing asymmetry may indicate nociceptive pain, comparable to pain on standing in people with OA. Central sensitization, resulting in abnormal central processing of pain signals, may additionally contribute to weight bearing asymmetry, and is the predominant mechanism underlying the lowering of mechanical thresholds at sites distal to the damaged joint. We found that increases in weight bearing asymmetry were more pronounced in the MNX model, whereas decreases in mechanical withdrawal thresholds distal to the joint damage better discriminated between arthritic and non-arthritic controls in the MIA model. These data suggest that the relative contributions of peripheral and central pain mechanisms may differ between these two models. Indeed, we have previously demonstrated a facilitation of spinal neuronal responses, which correlate with changes in the mechanical withdrawal thresholds in the hindpaw<sup>17</sup> in the MIA model and we have demonstrated the activation of neuroimmune cells in the spinal cord in this model<sup>15,31</sup>. The manifestation of spinal events in the MIA model supports the hypothesis that central sensitization contributes to pain responses in this model. In humans quantitative sensory testing shows lowering of pain pressure thresholds at both affected and remote sites<sup>14</sup> which map to the sites we see here<sup>32</sup>.

Based on these structural and behavioral differences between OA models, we hypothesized that synovitis may play a greater role in mediating pain behavior in the MNX model than in the MIA model. Consistent with this, intra-articular injection of triamcinolone acetonide, which reduced synovitis, reduced both weight bearing asymmetry and distal allodynia in the MNX model, but not in the MIA model. These data in particular indicate that mechanisms leading to the development of central sensitization may differ between models, and that synovitis may drive central sensitization in the MNX model of OA.

Rat models of induced OA display several advantages and limitations<sup>33</sup>. Amenability to pharmacological interventions, behavioral and structural assessment permits mechanistic studies that would be impossible in larger mammals or man due to cost and ethical considerations. However, the current study illustrates that MIA and MNX models do not mimic identical aspects of human disease. Previous comparisons have often depended on data collected from different models in separate experiments, or by different researchers. In the MNX model we showed no difference in paw withdrawal thresholds between MNX and sham animals in contrast to Fernihough *et al.*<sup>13</sup> and Bove<sup>11</sup>. However, details in the surgical procedure and method of reporting the data, respectively, may account for such differences. Similarly, we report no inflammation of the knee in the MIA model whereas others do when the dose of MIA is increased<sup>13,34</sup>. The extent of pain behavior may be affected by many factors, including structural severity<sup>8</sup> strain of rat<sup>35</sup> or housing conditions<sup>36</sup>, each of which may confound comparisons between models. Even in the current study the extent of distal allodynia in the MNX model was found to vary



between experiments. Furthermore, we and others have previously demonstrated significant weight bearing asymmetry in MIA-injected rats<sup>9,11</sup>. Clearly, in line with ARRIVE guidelines, it is important to report positive as well as negative findings and their variability so that it is evident how robust the models and endpoints are. However, our current findings demonstrate that when confounders are controlled for by concurrent experimentation, important differences in structural pathology, pain behavior and responses to an intervention were demonstrated between MNX and MIA models.

The lowering of hindpaw mechanical withdrawal thresholds in non-arthritic control rats may arise as a result of post-operative pain produced by the surgery as the medial and posterior articular nerves may be damaged during induction, and direct neurotoxicity has been reported with high doses of MIA<sup>37</sup>. Furthermore neuronal injury in the dorsal root ganglia following on from peripheral inflammation may also be a factor<sup>34,37,38</sup>. Clearly, nerve damage can lead to central sensitization, a key feature of neuropathic pain<sup>39</sup> and, therefore, it is essential that appropriate controls are employed to aid attribution of behavioral changes to OA.

## Conclusion

Our data provide evidence that both MIA and MNX models in rats resemble human OA, but that differences between the models should be taken into account when studying specific aspects of human disease. The models differed in important aspects of both structural pathology and pain behavior. Inflammation may play a greater role in the development of pain behavior in the MNX model, although in both models non-inflammatory mechanisms are likely to contribute. Judicious use of animal models should help elucidate not only mechanisms of human disease, but also inform the development and use of novel treatments. Treatments that relieve pain in all models may have more generalisable applicability to human arthritis pain, whilst those whose effects are model-specific may make important contributions to stratified care in the future.

## Author contributions

All the authors have made substantial contributions to:

The conception and design of the study, or acquisition of the data, or analysis and interpretation of the data.

The drafting of the article or revising it for important intellectual content and have approved the version of the article submitted.

## Role of the funding source

This study was funded by Arthritis Research UK Grant number 18769.

## Competing interest statement

The authors declare that they have no competing interests.

## References

- Mapp PI, Walsh DA, Bowyer J, Maciewicz RA. Effects of a metalloproteinase inhibitor on osteochondral angiogenesis, chondropathy and pain behavior in a rat model of osteoarthritis. *Osteoarthritis Cartilage* 2010;18(4):593–600.
- Yusuf E, Kortekaas MC, Watt I, Huizinga TW, Kloppenburg M. Do knee abnormalities visualised on MRI explain knee pain in knee osteoarthritis? A systematic review. *Ann Rheum Dis* 2011;70(1):60–7.
- Conaghan PG, Dickson J, Grant RL. Care and management of osteoarthritis in adults: summary of NICE guidance. *BMJ* 2008;336(7642):502–3.
- Bonnet CS, Walsh DA. Osteoarthritis, angiogenesis and inflammation. *Rheumatology (Oxford)* 2005;44(1):7–16.
- Janusz MJ, Bendele AM, Brown KK, Taiwo YO, Hsieh L, Heitmeyer SA. Induction of osteoarthritis in the rat by surgical tear of the meniscus: inhibition of joint damage by a matrix metalloproteinase inhibitor. *Osteoarthritis Cartilage* 2002;10(10):785–91.
- Mapp PI, Avery PS, McWilliams DF, Bowyer J, Day C, Moores S, et al. Angiogenesis in two animal models of osteoarthritis. *Osteoarthritis Cartilage* 2008;16(1):61–9.
- Wancket LM, Baragi V, Bove S, Kilgore K, Korytko PJ, Guzman RE. Anatomical localization of cartilage degradation markers in a surgically induced rat osteoarthritis model. *Toxicol Pathol* 2005;33(4):484–9.
- Guingamp C, Gegout-Pottie P, Philippe L, Terlain B, Netter P, Gillet P. Mono-iodoacetate-induced experimental osteoarthritis: a dose-response study of loss of mobility, morphology, and biochemistry. *Arthritis Rheum* 1997;40(9):1670–9.
- Combe R, Bramwell S, Field MJ. The monosodium iodoacetate model of osteoarthritis: a model of chronic nociceptive pain in rats? *Neurosci Lett* 2004;370(2–3):236–40.
- Dunham J, Hoedt-Schmidt S, Kalbhen DA. Prolonged effect of iodoacetate on articular cartilage and its modification by an anti-rheumatic drug. *Int J Exp Pathol* 1993;74(3):283–9.
- Bove SE, Calcaterra SL, Brooker RM, Huber CM, Guzman RE, Juneau PL, et al. Weight bearing as a measure of disease progression and efficacy of anti-inflammatory compounds in a model of monosodium iodoacetate-induced osteoarthritis. *Osteoarthritis Cartilage* 2003;11(11):821–30.
- Kalbhen DA. Chemical model of osteoarthritis—a pharmacological evaluation. *J Rheumatol* 1987;14. *Spec No*:130–1.
- Fernihough J, Gentry C, Malcangio M, Fox A, Rediske J, Pellas T, et al. Pain related behaviour in two models of osteoarthritis in the rat knee. *Pain* 2004;112(1–2):83–93.
- Suokas AK, Walsh DA, McWilliams DF, Condon L, Moreton B, Wylde V, et al. Quantitative sensory testing in painful osteoarthritis: a systematic review and meta-analysis. *Osteoarthritis Cartilage* 2012;20(10):1075–85.
- Sagar DR, Burston JJ, Hathway GJ, Woodhams SG, Pearson RG, Bennett AJ, et al. The contribution of spinal glial cells to chronic pain behaviour in the monosodium iodoacetate model of osteoarthritic pain. *Mol Pain* 2011;7:88.
- Gerwin N, Bendele AM, Glasson S, Carlson CS. The OARSI histopathology initiative – recommendations for histological assessments of osteoarthritis in the rat. *Osteoarthritis Cartilage* 2010;18(Suppl 3):S24–34.
- Sagar DR, Staniaszek LE, Okine BN, Woodhams S, Norris LM, Pearson RG, et al. Tonic modulation of spinal hyperexcitability by the endocannabinoid receptor system in a rat model of osteoarthritis pain. *Arthritis Rheum* 2010;62(12):3666–76.
- Wenham CY, Conaghan PG. The role of synovitis in osteoarthritis. *Ther Adv Musculoskelet Dis* 2010;2(6):349–59.
- Hill CL, Hunter DJ, Niu J, Clancy M, Guerhazi A, Genant H, et al. Synovitis detected on magnetic resonance imaging and its relation to pain and cartilage loss in knee osteoarthritis. *Ann Rheum Dis* 2007;66(12):1599–603.
- Dieppe PA, Lohmander LS. Pathogenesis and management of pain in osteoarthritis. *Lancet* 2005;365(9463):965–73.
- Hunskar S, Hole K. The formalin test in mice: dissociation between inflammatory and non-inflammatory pain. *Pain* 1987;30(1):103–14.
- Pomonis JD, Boulet JM, Gottshall SL, Phillips S, Sellers R, Bunton T, et al. Development and pharmacological characterization of a rat model of osteoarthritis pain. *Pain* 2005;114(3):339–46.

23. Ferland CE, Laverty S, Beaudry F, Vachon P. Gait analysis and pain response of two rodent models of osteoarthritis. *Pharmacol Biochem Behav* 2011;97(3):603–10.
24. Blom AB, van Lent PL, Holthuysen AE, van der Kraan PM, Roth J, van Rooijen N, et al. Synovial lining macrophages mediate osteophyte formation during experimental osteoarthritis. *Osteoarthritis Cartilage* 2004;12(8):627–35.
25. van Lent PL, Blom AB, van der Kraan P, Holthuysen AE, Vitters E, van Rooijen N, et al. Crucial role of synovial lining macrophages in the promotion of transforming growth factor beta-mediated osteophyte formation. *Arthritis Rheum* 2004;50(1):103–11.
26. Suri S, Gill SE, Massena de Camin S, Wilson D, McWilliams DF, Walsh DA. Neurovascular invasion at the osteochondral junction and in osteophytes in osteoarthritis. *Ann Rheum Dis* 2007;66(11):1423–8.
27. Walsh DA, Bonnet CS, Turner EL, Wilson D, Situ M, McWilliams DF. Angiogenesis in the synovium and at the osteochondral junction in osteoarthritis. *Osteoarthritis Cartilage* 2007;15(7):743–51.
28. Strassle BW, Mark L, Leventhal L, Piesla MJ, Jian Li X, Kennedy JD, et al. Inhibition of osteoclasts prevents cartilage loss and pain in a rat model of degenerative joint disease. *Osteoarthritis Cartilage* 2012;18(10):1319–28.
29. Walsh DA, McWilliams DF, Turley MJ, Dixon MR, Franses RE, Mapp PI, et al. Angiogenesis and nerve growth factor at the osteochondral junction in rheumatoid arthritis and osteoarthritis. *Rheumatology (Oxford)* 2012;49(10):1852–61.
30. Hwang J, Bae WC, Shieu W, Lewis CW, Bugbee WD, Sah RL. Increased hydraulic conductance of human articular cartilage and subchondral bone plate with progression of osteoarthritis. *Arthritis Rheum* 2008;58(12):3831–42.
31. Lee Y, Pai M, Brederson JD, Wilcox D, Hsieh G, Jarvis MF, et al. Monosodium iodoacetate-induced joint pain is associated with increased phosphorylation of mitogen activated protein kinases in the rat spinal cord. *Mol Pain* 2011;7:39.
32. Hendiani JA, Westlund KN, Lawand N, Goel N, Lisse J, McNearney T. Mechanical sensation and pain thresholds in patients with chronic arthropathies. *J Pain* 2003;4(4):203–11.
33. Vincent TL, Williams RO, Maciewicz R, Silman A, Garside P. Mapping pathogenesis of arthritis through small animal models. *Rheumatology (Oxford)* 2012;51(11):1931–41.
34. Orita S, Ishikawa T, Miyagi M, Ochiai N, Inoue G, Eguchi Y, et al. Pain-related sensory innervation in monoiodoacetate-induced osteoarthritis in rat knees that gradually develops neuronal injury in addition to inflammatory pain. *BMC Musculoskelet Disord* 2011;12:134.
35. Yoon YW, Lee DH, Lee BH, Chung K, Chung JM. Different strains and substrains of rats show different levels of neuropathic pain behaviors. *Exp Brain Res* 1999;129(2):167–71.
36. Rossi HL, Neubert JK. Effects of environmental enrichment on thermal sensitivity in an operant orofacial pain assay. *Behav Brain Res* 2008;187(2):478–82.
37. Ferreira-Gomes J, Adaes S, Sousa RM, Mendonca M, Castro-Lopes JM. Dose-dependent expression of neuronal injury markers during experimental osteoarthritis induced by monoiodoacetate in the rat. *Mol Pain* 2012;8:50.
38. Ivanavicius SP, Ball AD, Heapy CG, Westwood FR, Murray F, Read SJ. Structural pathology in a rodent model of osteoarthritis is associated with neuropathic pain: increased expression of ATF-3 and pharmacological characterisation. *Pain* 2007;128(3):272–82.
39. Seltzer Z, Dubner R, Shir Y. A novel behavioral model of neuropathic pain disorders produced in rats by partial sciatic nerve injury. *Pain* 1990;43(2):205–18.